Received: 14 February 2020 | Revised: 7 February 2021 | Accepted: 10 May 2021

DOI: 10.1002/rnc.5607

RESEARCH ARTICLE

WILEY

Immersion and invariance-based extended state observer design for a class of nonlinear systems

Mehran Hosseini-Pishrobat[1] | **Jafar Keighobadi**[1] | **Armin Pirastehzad**[2] | **Mohammad Javad Yazdanpanah**[2]

[1]Faculty of Mechanical Engineering, University of Tabriz, Tabriz, Iran

[2]Control and Intelligent Processing Center of Excellence, School of Electrical and Computer Engineering, University of Tehran, Tehran, Iran

Correspondence
Jafar Keighobadi, Faculty of Mechanical Engineering, University of Tabriz, 29 Bahman, P.C. 5166614766, Tabriz, Iran.
Email: Keighobadi@tabrizu.ac.ir

Abstract

This article presents a novel geometric framework for the design of extended state observers (ESOs) using the immersion and invariance (I&I) method. The ESO design problem of a class of uncertain lower-triangular nonlinear systems is considered for joint state and total disturbance observation. This problem is formulated as designing a dynamical system, as the observer, along with an appropriately defined manifold in the system-observer extended state-space. The ESO convergence translates into the attractivity of this manifold; that is, the convergence of the system-observer trajectories to a small boundary layer around the manifold. The design of both reduced-order and full-order ESOs is studied using the I&I formulation. Moreover, an optimization method based on linear matrix inequalities is proposed to establish the convergence of ESOs. It is shown that the I&I-based method leads to a unifying framework for the design and analysis of ESOs with linear, nonlinear, and time-varying gains. Detailed simulations are provided to show the efficacy of the proposed ESOs.

KEYWORDS

disturbance, extended state observer, immersion and invariance, linear matrix inequality, nonlinear systems

1 | INTRODUCTION

Extended state observers (ESOs) are observers that estimate the total disturbance perturbing a given system along with its state variables. The total disturbance stands for the mismatch between the physical system and the corresponding mathematical model, and, in general, it is a function of the state variables and unknown external inputs.[1,2] This definition encompasses a large class of disturbances and uncertainties such as parameter variations, unmodeled dynamics, external disturbances, and noises. Hence, ESOs, as effective tools for disturbance estimation, lie at the core of active disturbance rejection control (ADRC) methods.[1-4] ESOs can be also used to robustify the existing control methods against wider classes of disturbances while removing the need for full-state measurement.[5,6]

The core idea of ESOs is to augment an approximate dynamical model of the total disturbance (usually an integral action) to the underlying system's dynamics and subsequently design an observer for the resultant extended system. Following the seminal works of Han,[1,2] the problems of design and convergence analysis of ESOs, for effective disturbance estimation, have been studied intensively. As one of the first rigorous studies of the subject, the convergence of high-gain ESOs has been investigated by Guo and Zhao[7] for fully feedback linearizable, single-input, single-output (SISO) systems subjected to uncertainty and disturbances. Extending the results from continuous-time to discrete-time for the same class of systems, the convergence and performance of discrete-time nonlinear ESOs have been investigated as well.[8] For a class of uncertain SISO nonlinear systems in the lower-triangular form, constant gain and time-varying gain ESOs have been designed and assessed.[9] For the same type of systems, the convergence of a class of ESOs that employ fractional power gain functions has been studied;[10] it was highlighted that these ESOs offer better measurement noise immunity and smaller peaking values with respect to the linear ESOs. These results have been further extended to a more general class of multi-input multi-output nonlinear systems with mismatched uncertainty.[11] A convex optimization-based method has been proposed to establish the convergence of an ESO with dead-zone-type nonlinear gain functions.[5] A more involved model of the total disturbance dynamics, instead of the commonly used integral action, has been applied to improve the disturbance estimation quality of a nonlinear ESO.[6]

The term “immersion and invariance” (I&I) refers to a class of geometric design methods relying upon system immersion and manifold invariance. For a given system, the fundamental I&I design steps are as follows.[12,13] First, find an invariant manifold with the property that the system trajectories evolving on this manifold fulfill the design objectives; this amounts to immersing the system into its reduced-order dynamics on the manifold. Second, make the invariant manifold locally or globally attractive to satisfy the design objectives over the domain of interest in the state-space. This method is extended to present a new formulation of the observer design problem of nonlinear systems.[13,14] In this regard, the observer design problem of a given system is recast as the problem of designing an attractive, invariant manifold in the joint system-observer state-space. With respect to the Luenberger-type and Lie-algebraic-based methods, this formulation enables the design of asymptotic, reduced-order observers under milder conditions on the system nonlinearities.[13,14] The generality of the I&I formulation of the observer design problem, in connection with the Luenberger-type observers, is shown by Ortega and Zhang.[15] I&I observers have been proposed and studied for a wide variety of applications such as Euler–Lagrange systems,[13,16] nonholonomic mechanical systems,[17] nonlinear vibrating systems,[18] attitude-heading reference systems,[19] and systems with time-delayed measurements.[20]

The main contribution of this article is to present a geometric framework for the ESO design. We consider uncertain nonlinear systems admitting the lower-triangular form. The novelties and distinctive features of this design method, with respect to the existing ones, are as follows.

- Existing approaches for the ESO design, essentially, follow the framework of the Luenberger observers. More specifically, these ESOs duplicate the mathematical structure of the system’s equations and add feedback terms of the output estimation error. Then, a stability criterion is applied to analyze the corresponding estimation error dynamics and to examine the convergence of the state/total disturbance estimation, accordingly. From a geometric vantage point, this corresponds to the stabilization of the zero estimation error manifold in the joint system-observer state-space. Our approach differs from this paradigm in the sense that neither the structure of the ESO nor the desired manifold is given in prior, but they are derived by a design process. We achieve this in a constructive manner by setting up an invariant manifold and rendering it attractive for the system-observer trajectories. Similar to the seminal work of Karagiannis et al.,[14] the I&I formulation provides a novel definition and interpretation of the convergence of an ESO.
- Compared with the original works on I&I observers,[13,14] the novelty of our approach lies in the inclusion of uncertainty. Invoking the notion of set-attractivity, we present a modified definition for an I&I observer that takes into account the effect of disturbances and uncertainty on the system trajectories. In this setting, we prove that the trajectories convergence to a boundary layer around the target manifold.
- We study both reduced-order and full-order ESO design problems. We note that the original definition of an I&I observer is given in the reduced-order design framework.[14] Hence, we extend the definition to include full-order state estimation. The underlying motivation for considering the full-order case is to incorporate a mechanism of estimation error feedback into the observer dynamics as in conventional ESOs. We show that such a feedback mechanism differs from that of the conventional ESOs because of the I&I design.
- The proposed method presents a unifying framework for the design and analysis of ESOs with linear, nonlinear, and time-varying gains. The convergence analysis results hold for a large class of bounded gain functions satisfying a Lyapunov-type inequality. On this basis, we use linear matrix inequalities (LMIs) to present an optimization-based method to establish the ESO convergence.

The rest of the article is organized as follows. Section 2 briefly reviews notation and mathematical preliminaries. Section 3 formulates the ESO design problem. Sections 4 presents the main results for both reduced-order and full-order ESO designs. Section 5 proposes an LMI-based method to establish the convergence of the ESOs and, also, discusses some special design cases. Section 6 presents illustrative numerical simulations, and Section 7 concludes the article.

2 | NOTATION AND PRELIMINARIES

Throughout this article, $\mathbb{R}_{\geq 0}$ denotes the set of nonnegative real numbers. For two sets A and B, $A \times B$ is their Cartesian product. We consider the Euclidean space $\mathbb{R}^n$ endowed with its standard topology. For a set $(.) \subseteq \mathbb{R}^n$, we denote its interior by int(.). $\|.\|$ stands for the two-norm of a vector as well as the corresponding induced matrix norm. For a real symmetric matrix P, $P > 0\ (\geq 0)$ and $P < 0\ (\leq 0)$ means that P is positive definite (positive semidefinite) and negative definite (negative semidefinite), respectively. The smallest and the largest eigenvalues of P are denoted by $\lambda_{\min}(P)$ and $\lambda_{\max}(P)$, respectively. $C^0(A, B)$ and $C^1(A, B)$ denote the set of functions $f : A \rightarrow B$ that are continuous and continuously differentiable over A, respectively. col(., ., ...) is the vector stacked by the given vectors in its argument. The Kronecker delta is denoted by δ_{ij} where $\delta_{ij} = 1$ for $i = j$, and $\delta_{ij} = 0$ for $i \neq j$. The notation $i = 1 : n$ means that the index i takes all the integer values from 1 to n.

Consider the dynamical system

$$\dot{\chi}(t) = q(\chi(t), t), \tag{1}$$

where $\chi \in \mathcal{X}$ is the state vector, with $\mathcal{X} \subseteq \mathbb{R}^n$ being a connected n-dimensional manifold, and $q(.) \in \mathbb{R}^n$ is a sufficiently regular function such that the existence and uniqueness of the system trajectories are guaranteed for all $t \in \mathbb{R}_{\geq 0}$. In the (χ, t) space, we consider an m-dimensional $(m < n + 1)$ manifold $\mathcal{M} \subset \mathbb{R}^{n+1}$ such that $\mathcal{M} \cap (\text{int}(\mathcal{X}) \times \mathbb{R}_{\geq 0}) \neq \emptyset$. An *off-the-manifold coordinate*[13] with respect to $\mathcal{M}$, $z(t) := \bar{z}(\chi(t), t)$, $\bar{z} \in C^1(\mathbb{R}^n \times \mathbb{R}_{\geq 0}, \mathbb{R}^{n_z})$, is a measure of the distance of trajectories of system (1) from $\mathcal{M}$. Mathematically, $z(t) = 0$, for all $t \in \mathbb{R}_{\geq 0}$, if and only if $(\chi(t), t) \in \mathcal{M}$, for all $t \in \mathbb{R}_{\geq 0}$. For a positive r, define the set

$$\Lambda_r := \left\{ (\chi, t) \in \mathcal{X} \times \mathbb{R}_{\geq 0} \middle| \|\bar{z}(\chi, t)\| \leq r \right\}, \tag{2}$$

which can be understood as a boundary layer engulfing $\mathcal{M}$ over $\mathcal{X} \times \mathbb{R}_{\geq 0}$.

Definition 1. Regarding the trajectories of system (1), we define the following properties for the manifold $\mathcal{M}$:

P1. Positive invariance: If $z(t_0) = 0$, then $z(t) = 0$ for all $t \geq t_0$, $t_0 \in \mathbb{R}_{\geq 0}$.
P2. Attractivity: For all $t_0 \in \mathbb{R}_{\geq 0}$, there exists a positive r such that if $z(t_0) \in \Lambda_r$, then $z(t)$ remains bounded for all $t \geq t_0$ and $\lim_{t\to\infty} \|z(t)\| = 0$.
P3. Λ_r-attractivity: For all $t_0 \in \mathbb{R}_{\geq 0}$, there exists a positive r_0 such that if $z(t_0) \in \Lambda_{r_0}$, then $z(t)$ remains bounded for all $t \geq t_0$ and furthermore, there exist a positive r_1 and a finite reaching time $t_r = t_r(r_0, r_1) > 0$ in a way that $z(t) \in \Lambda_{r_1}$ for all $t \geq t_0 + t_r$.

We note that the intuition behind the definition of Λ_r-attractivity stems from the notion of practical stability in the sense of uniform ultimate boundedness.[21,22] That is, the trajectories of system (1) converge to a boundary layer around the manifold $\mathcal{M}$. This enables us to handle the effects of model uncertainty and disturbances in I&I observer design problems.

3 | PROBLEM FORMULATION

In this article, we consider an n-dimensional lower-triangular nonlinear system of the form

$$\begin{aligned} \dot{\zeta}_i(t) &= \zeta_{i+1}(t) + f_i(\zeta_1(t), \ldots, \zeta_i(t), u(t)), \ i = 1 : n-1, \\ \dot{\zeta}_n(t) &= f_n(\zeta_1(t), \ldots, \zeta_n(t), u(t)) + g(\zeta_1(t), \ldots, \zeta_n(t), w(t)), \end{aligned} \tag{3}$$

where $\zeta_i \in \mathbb{R}$ are the state variables, $u \in C^1(\mathbb{R}_{\geq 0}, \mathbb{R})$ is the known input, $w \in C^1(\mathbb{R}_{\geq 0}, \mathbb{R})$ is the unknown disturbance input, $f_i \in C^0(\mathbb{R}^{i+1}, \mathbb{R})$ are known nonlinear functions that represent the nominal part of the system dynamics, and $g \in C^0\left(\mathbb{R}^{n+1}, \mathbb{R}\right)$ is an unknown nonlinear function representing the uncertain dynamics of the system. Following the terminology of the ADRC literature, we refer to the function $g(.)$ as the *total disturbance* of system (3).

Assumption 1. System (3) satisfies the following requirements:

(i) The functions $f_i(.)$, $i = 1 : n$, are locally Lipschitz continuous with respect to ζ_j, $j = 1 : i$, and $g(.)$ is differentiable with respect to its arguments;
(ii) There exists a positive u_0 such that $|u(t)| \leq u_0$ for all $t \in \mathbb{R}_{\geq 0}$;
(iii) There exist positive numbers w_1 and w_2 such that $|w(t)| \leq w_1$ and $|\dot{w}(t)| \leq w_2$ for all $t \in \mathbb{R}_{\geq 0}$;
(iv) All trajectories $\zeta_i(t)$, $t \in \mathbb{R}_{\geq 0}$, belong to a compact set $\Omega \subset \mathbb{R}^n$.

Considering ζ_1 as the measured output of system (3), we are interested in the problem of extended state observation. That is, our goal is to estimate both the state variables $\zeta_i \in \mathbb{R},\ i = 1 : n$, and the total disturbance $g(.)$. Accordingly, we introduce the following variables:

$$
\begin{aligned}
y &= \zeta_1, \\
x_i &= \zeta_{i+1},\ i = 1 : n-1, \\
x_n &= g\left(y, x_1, \ldots, x_{n-1}, w\right),
\end{aligned} \tag{4}
$$

where $y \in \mathbb{R}$ is the measured state variable of the system, $x_i \in \mathbb{R}, i = 1 : n-1$ are the unmeasured state variables, and $x_n \in \mathbb{R}$ is the extended state variable corresponding to the total disturbance. As per the new variables (4), by introducing the vectors

$$
\begin{aligned}
\overline{x}_i &:= [x_1, \ldots, x_i]^\top \in \mathbb{R}^i,\ i = 1 : n, \\
x &= \overline{x}_n \in \mathbb{R}^n,
\end{aligned} \tag{5}
$$

we transform system (3) into the following extended system:

$$
\begin{aligned}
\dot{y}(t) &= Cx(t) + f_1\left(y(t), u(t)\right), \\
\dot{x}(t) &= Ax(t) + \sum_{i=1}^{n-1} B_i f_{i+1}\left(y(t), \overline{x}_i(t), u(t)\right) + B_n h\left(y(t), x(t), u(t), w(t), \dot{w}(t)\right),
\end{aligned} \tag{6}
$$

where the system matrices are defined as

$$
A = \begin{bmatrix} 0 & 1 & 0 & \ldots & 0 \\ 0 & 0 & 1 & \ldots & 0 \\ \vdots & \vdots & \vdots & \ddots & \vdots \\ 0 & 0 & 0 & \ldots & 1 \\ 0 & 0 & 0 & \ldots & 0 \end{bmatrix} \in \mathbb{R}^{n \times n},\ B_i = \begin{bmatrix} \delta_{1i} \\ \vdots \\ \delta_{ni} \end{bmatrix} \in \mathbb{R}^{n \times 1},\ C = \begin{bmatrix} 1 & 0 & \ldots & 0 \end{bmatrix} \in \mathbb{R}^{1 \times n},\ i = 1 : n,
$$

and

$$
\begin{aligned}
h\left(y, x, u, w, \dot{w}\right) := {} & \frac{\partial g\left(y, \overline{x}_{n-1}, w\right)}{\partial y}\left(x_1 + f_1\left(y, u\right)\right) + \sum_{i=1}^{n-1} \frac{\partial g\left(y, \overline{x}_{n-1}, w\right)}{\partial x_i}\left(x_{i+1} + f_{i+1}\left(y(t), \overline{x}_i(t), u(t)\right)\right) \\
& + \frac{\partial g\left(y, \overline{x}_{n-1}, w\right)}{\partial w}\dot{w}.
\end{aligned} \tag{7}
$$

Similar to the works of Zhao and Guo,[3,7] we make the following assumption on the function $h(.)$ to facilitate the subsequent stability analyses.

Assumption 2. There exists a positive function $\varrho \in C^0\left(\mathbb{R}^{n+1}, \mathbb{R}_{\geq 0}\right)$ such that the following inequality holds for all $\left(y, \bar{x}_{n-1}, w\right) \in \mathbb{R}^{n+1}$;

$$\left|\frac{\partial g\left(y, \bar{x}_{n-1}, w\right)}{\partial y}\right| + \sum_{i=1}^{n-1}\left|\frac{\partial g\left(y, \bar{x}_{n-1}, w\right)}{\partial x_i}\right| + \left|\frac{\partial g\left(y, \bar{x}_{n-1}, w\right)}{\partial w}\right| \leq \varrho\left(y, \bar{x}_{n-1}, w\right). \tag{8}$$

Remark 1. Establishing the convergence of an ESO requires some regularity and boundedness conditions on the total disturbance and its time derivative.[3,7,9] Hence, we made Assumption 1, parts (iii) and (iv), and Assumption 2. Part (iv) of Assumption 1 can be relaxed at the expense of loss of generality. For example, if the total disturbance depended only on w, then part (iii) of Assumption 1 would be sufficient. From a control perspective, when an ESO is integrated with a nominal, stabilizing full-state feedback controller in a certainty equivalence fashion, the semiglobal practical stability of the corresponding closed-loop system can be established by the separation principle.[3] In such a case, no prior assumption on the boundedness of the state variables is required.

Remark 2. According to parts (iii) and (iv) of Assumption 1–along with the continuity of $g(.)$–there exists a positive g_0 such that $|x_n(t)| \leq g_0$, for all $t \in \mathbb{R}_{\geq 0}$. Therefore, the trajectories of the extended system (6) belong to the compact set $\Omega_{\text{ext}} := \Omega \times [-g_0, g_0]$.

Remark 3. We present our ESO design method for the systems admitting the lower-triangular form (3). Transformation of general nonlinear systems with external inputs to canonical lower-triangular forms is possible under suitable conditions characterized by differential observability and uniform observability. For example, if the output and its first $n-1$ Lie derivatives of an input-affine system form a diffeomorphism (n is the dimension of the state-space), then such a transformation exists.[23,24] For a thorough discussion of this topic, we refer the reader to Gauthier and Kupka,[23] Bernard et al.,[24] and the recent book by Bernard.[25]

4 | MAIN RESULTS

4.1 | Reduced-order ESO design

In this section, we consider the problem of reduced-order extended state observation that entails estimation of the unmeasured states of the extended system (6). To put the problem in perspective, we first present the definition of a reduced-order observer in the sense of I&I.[13,14] This definition forms the departure point of our design method.

Definition 2 (Reduced-order observer). Consider a dynamical system of the form

$$\dot{\xi} = \alpha(\xi, y, u, t), \tag{9}$$

where $\xi \in \mathbb{R}^n$ and $\alpha \in C^1\left(\mathbb{R}^{n+3}, \mathbb{R}^n\right)$. System (9) is called a reduced-order observer for the extended system (6) if there exist mappings $\phi_1 \in C^1\left(\mathbb{R}^{n+3}, \mathbb{R}^n\right)$ and $\beta_1 \in C^1\left(\mathbb{R}^{n+3}, \mathbb{R}^n\right)$ such that ϕ_1 is left-invertible with respect to x and the C^1 manifold

$$\mathcal{M}_1 := \left\{(y, x, \xi, u, t) \in \mathbb{R}^{2n+3} | \phi_1(x, y, u, t) = \beta_1(\xi, y, u, t)\right\} \tag{10}$$

satisfies the properties P1 and P2 with respect to systems (6) and (9) for all $(y, x, \xi, u, t) \in \mathcal{X}_1 \times \mathbb{R}_{\geq 0}$, where $\mathcal{X}_1 \subset \Omega_{ext} \times \mathbb{R}^n \times [-u_0, u_0]$ is a connected $2n+2$-dimensional manifold.

Remark 4. According to Definition 2, an asymptotically convergent estimate of the unmeasured state variables is given by

$$\hat{x} = \phi_1^L\left(\beta_1(\xi, y, u, t), y, u, t\right), \tag{11}$$

where ϕ_1^L is a left-inverse of the mapping ϕ_1, that is, $\phi_1^L(\phi_1(x, y, u, t), y, u, t) = x$ for all $(x, y, u, t) \in \mathbb{R}^{n+3}$.[13] The observer is reduced-order because its dimension, n is lower than the dimension of system (6), $n+1$.

The main issue that arises when we try to use Definition 2 to solve the reduced-order ESO design problem is the presence of the unknown function $h(.)$. More specifically, the time derivative of the total disturbance induces uncertainty in the dynamics of the system–on the manifold $\mathcal{M}_1$–that precludes the properties P1 and P2. We note that even though the effect of the known functions $f_i(.)$–due to their Lipschitz continuity–can be compensated, full compensation of the effect of $h(.)$ is not possible in general. Therefore, to relax the strict requirements of the I&I observer, we combine the notion of Λ_r-attractivity with Definition 2 to present a geometric definition of a reduced-order ESO.

Definition 3 (Reduced-order ESO). Consider the mathematical setting of Definitions 1 and 2, and, in Definition 2, replace the properties P1 and P2 of the manifold $\mathcal{M}_1$ with the property P3 of Λ_r-attractivity for some $r_0 > 0$. Moreover, assume that for any positive $r_1 < r_0$ there exist observer parameters rendering $\mathcal{M}_1$ Λ_r-attractive. Then, system (9) is called a reduced-order ESO for the extended system (6).

By Definition 3, we formulate the problem of reduced-order ESO design for system (6) as the problem of constructing a dynamical system of the form (9) along with a Λ_r-attractive manifold defined by (10). We assume that the mapping ϕ_1 is of the form

$$\phi_1(x, y, u, t) = x + \psi_1(y, u, t), \tag{12}$$

where $\psi_1 \in C^1\left(\mathbb{R}^3, \mathbb{R}^n\right)$. Hence, the manifold (10) becomes

$$\mathcal{M}_1 := \left\{(y, x, \xi, u, t) \in \mathbb{R}^{2n+3} | x + \psi_1(y, u, t) = \beta_1(\xi, y, u, t)\right\}. \tag{13}$$

Introducing

$$\eta_1(\xi, y, u, t) := \beta_1(\xi, y, u, t) - \psi_1(y, u, t), \tag{14}$$

we use the following off-the-manifold coordinate to characterize the distance of the trajectories of systems (6) and (9) from $\mathcal{M}_1$:

$$z := x - \eta_1(\xi, y, u, t). \tag{15}$$

Remark 5. The off-the-manifold coordinate z measures the attractivity of $\mathcal{M}_1$. Moreover, according to Remark 4, a practical, asymptotic estimate of x is $\hat{x} = \eta_1(\xi, y, u, t)$ implying that $x - \hat{x} = z$. Therefore, the off-the-manifold coordinate z is also a direct measure of the state estimation error.

The off-the-manifold dynamics is given by

$$\begin{aligned}\dot{z}(t) = {} & \left(A - \frac{\partial \eta_1}{\partial y} C\right) z(t) + \left(A - \frac{\partial \eta_1}{\partial y} C\right) \eta_1(\xi(t), y(t), u(t), t) + \sum_{i=1}^{n-1} B_i f_{i+1}\left(y(t), \overline{x}_i(t), u(t)\right) \\ & + B_n h(y(t), x(t), u(t), w(t), \dot{w}(t)) - \frac{\partial \eta_1}{\partial y} f_1(y(t), u(t)) - \frac{\partial \eta_1}{\partial u} \dot{u}(t) - \frac{\partial \eta_1}{\partial t} - \frac{\partial \eta_1}{\partial \xi} \alpha(\xi(t), y(t), u(t), t).\end{aligned} \tag{16}$$

Assumption 3. For all $(\xi, y, u, t) \in \mathbb{R}^{n+3}$, $\det(\partial \eta_1 / \partial \xi)$ is bounded away from zero.

According to (16) and the invertibility of $(\partial \eta_1 / \partial \xi)$ by Assumption 3, we select the following observer dynamics:

$$\alpha(\xi, y, u, t) = \left(\frac{\partial \eta_1}{\partial \xi}\right)^{-1} \left(\left(A - \frac{\partial \eta_1}{\partial y} C\right) \eta_1(\xi, y, u, t) + \sum_{i=1}^{n-1} B_i f_{i+1}\left(y, \hat{\overline{x}}_i, u\right) - \frac{\partial \eta_1}{\partial y} f_1(y, u) - \frac{\partial \eta_1}{\partial u} \dot{u} - \frac{\partial \eta_1}{\partial t}\right), \tag{17}$$

where $\hat{x} = \eta_1$ and $\hat{\overline{x}}_i$ is defined componentwise according to $\hat{x}$. Thereby,

$$\begin{aligned}\dot{z}(t) = {} & \left(A - \frac{\partial \eta_1}{\partial y} C\right) z(t) + \sum_{i=1}^{n-1} B_i \left(f_{i+1}\left(y(t), \overline{x}_i(t), u(t)\right) - f_{i+1}\left(y(t), \hat{\overline{x}}_i(t), u(t)\right)\right) \\ & + B_n h(y(t), x(t), u(t), w(t), \dot{w}(t)).\end{aligned} \tag{18}$$

Assumption 4. There exist a positive definite matrix $P_1 \in \mathbb{R}^{n\times n}$ and a positive ϵ_1 such that the following matrix inequality holds for all $(\xi, y, u, t) \in \mathbb{R}^{n+3}$:

$$P_1\left(A - \frac{\partial \eta_1}{\partial y}C\right) + \left(A - \frac{\partial \eta_1}{\partial y}C\right)^\top P_1 + \frac{2}{\epsilon_1}P_1 \le 0. \tag{19}$$

Theorem 1. *Consider the extended system (6) and assume that Assumptions 1–4 are satisfied. System (9) with dynamics (17) is a reduced-order ESO–in the sense of Definition 3–for system (6), and the corresponding asymptotic state estimate is given by $\hat{x} = \eta_1(\xi, y, u, t)$.*

Proof. We present the proof by the following steps:

Step 1. Following Assumption 4, we consider a positive definite function of the form

$$V_1(z) := z^\top P_1 z, \tag{20}$$

and differentiate it with respect to time, along the trajectories of (18), to obtain

$$\begin{aligned}\dot{V}_1(z(t)) \le& -\frac{2}{\epsilon_1}V_1(z(t)) + 2z^\top(t)\sum_{i=1}^{n-1} P_1 B_i \left(f_{i+1}\left(y(t), \overline{x}_i(t), u(t)\right) - f_{i+1}\left(y(t), \hat{\overline{x}}_i(t), u(t)\right)\right)\\ &+ 2z^\top(t)P_1 B_n h\left(y(t), x(t), u(t), w(t), \dot{w}(t)\right).\end{aligned} \tag{21}$$

Step 2. By Assumption 2 and Equation (7), the absolute value of the function $h(.)$ is upper bounded by a continuous function. Hence, according to part (iii) of Assumption 1, there exists a positive h_0 such that

$$|h(y, x, u, w, \dot{w})| \le h_0, \tag{22}$$

for all $(y, x, u, w, \dot{w}) \in \Omega_{\text{ext}} \times [-u_0, u_0] \times \mathbb{R}^2$.

In the ξ space, let us consider a compact set $\Omega_\xi \subset \mathbb{R}^n$ such that the set $\mathcal{X}_1 := \Omega_{\text{ext}} \times \Omega_\xi \times [-u_0, u_0]$ satisfies $\mathcal{M}_1 \cap (\text{int}(\mathcal{X}_1) \times \mathbb{R}_{\ge 0}) \ne \emptyset$. The existence of such a Ω_ξ is guaranteed by the implicit function theorem.[26] By part (i) of Assumption 1, there exist positive constants l_{fi} such that the following inequalities hold for all $(y, x, \xi, u) \in \mathcal{X}_1$:

$$\|f_i(y, \overline{x}_{i-1}, u) - f_i(y, \hat{\overline{x}}_{i-1}, u)\| \le l_{fi}\|z\|,\ i = 2 : n. \tag{23}$$

Taking into account (22) and (23), the differential inequality (21) results in

$$\dot{V}_1(z(t)) \le -\left(\frac{2}{\epsilon_1} - 2l_f\frac{\lambda_{\max}(P_1)}{\lambda_{\min}(P_1)}\right)V_1(z(t)) + 2h_0\frac{\lambda_{\max}(P_1)}{\sqrt{\lambda_{\min}(P_1)}}\sqrt{V_1(z(t))}, \tag{24}$$

where $l_f := \sum_{i=2}^n l_{fi}$.

Step 3. Considering $\mathcal{X}_1$ as the connected manifold of interest, we examine the conditions of Definitions 1 and 3 to show the Λ_r-attractivity of $\mathcal{M}_1$. Assuming that

$$\epsilon_1 < \epsilon_1' := \frac{\lambda_{\min}(P_1)}{l_f\lambda_{\max}(P_1)}, \tag{25}$$

applying the comparison lemma to (24) results in

$$\|z(t)\| \le \sqrt{\frac{\lambda_{\max}(P_1)}{\lambda_{\min}(P_1)}}\left(\|z(t_0)\| - \sqrt{\frac{\lambda_{\max}(P_1)}{\lambda_{\min}(P_1)}}\lambda(\epsilon_1)h_0\right)\exp\left(-\frac{t-t_0}{\lambda(\epsilon)}\right) + \frac{\lambda_{\max}(P_1)}{\lambda_{\min}(P_1)}\lambda(\epsilon_1)h_0, \tag{26}$$

for all $t_0 \in \mathbb{R}_{\ge 0}$, $t \ge t_0$, where

$$\lambda(\epsilon_1) := \frac{\epsilon_1}{1 - \frac{\epsilon_1}{\epsilon_1'}}. \tag{27}$$

Assume $z(t_0) \in \Lambda_{r_0}$, for a positive r_0, and consider the positive numbers r_1, r_2 satisfying $r_2 < r_1 < r_0$. The inequality (26) shows that the trajectories starting in Λ_{r_0} remain bounded. In addition, defining a reaching time of the form

$$t_r := \lambda(\epsilon_1) \ln \left(\frac{1}{r_2} \sqrt{\frac{\lambda_{\max}(P_1)}{\lambda_{\min}(P_1)}} \left| \|z(t_0)\| - \sqrt{\frac{\lambda_{\max}(P_1)}{\lambda_{\min}(P_1)}} \lambda(\epsilon_1) h_0 \right| \right) \tag{28}$$

and assuming that

$$\epsilon_1 < \epsilon_1'' := \frac{r_1 - r_2}{h_0 \frac{\lambda_{\max}(P_1)}{\lambda_{\min}(P_1)} + \frac{r_1 - r_2}{\epsilon_1'}}, \tag{29}$$

we conclude that $z(t) \in \Lambda_{r_1}$, for all $t \geq t_0 + t_r$. Noting that $\epsilon_1'' < \epsilon_1'$, if the condition (29) holds, the manifold $\mathcal{M}_1$ is Λ_r-attractive for any positive $r_1 < r_0$. Therefore, system (9) with dynamics (17) is a reduced-order ESO for the extended system (6). ■

Corollary 1. *If Theorem 1 holds, then* $\overline{\lim}_{\substack{t \to \infty \\ \epsilon_1 \to 0}} \|z(t)\| = 0$.

Proof. Considering Equation (26), we have

$$\overline{\lim_{t \to \infty}} \|z(t)\| \leq \frac{\lambda_{\max}(P_1)}{\lambda_{\min}(P_1)} \lambda(\epsilon_1) h_0. \tag{30}$$

Since $\lambda(\epsilon_1) = O(\epsilon_1)$ as $\epsilon_1 \to 0$, the ultimate bound of $\|z(.)\|$ goes to zero as $\epsilon_1 \to 0$. ■

4.2 | Full-order ESO design

In this section, we study the problem of full-order extended state observation for system (6). That is, we aim to estimate both measured and unmeasured state variables. In this regard, we first present an I&I-based definition for the full-order observer that forms the basis of the full-order ESO design.

Definition 4 (Full-order observer). Consider a dynamical system of the form

$$\begin{aligned} \dot{\hat{y}}(t) &= \alpha_1 \left(\hat{y}(t), \xi(t), y(t), u(t), t\right), \\ \dot{\xi}(t) &= \alpha_2 \left(\hat{y}(t), \xi(t), y(t), u(t), t\right), \end{aligned} \tag{31}$$

where $(\hat{y}, \xi) \in \mathbb{R}^{n+1}$, $\alpha_1 \in C^1\left(\mathbb{R}^{n+4}, \mathbb{R}\right)$, and $\alpha_2 \in C^1\left(\mathbb{R}^{n+4}, \mathbb{R}^n\right)$. System (31) is called a full-order observer for the extended system (6) if there exist mappings $\phi_2 \in C^1\left(\mathbb{R}^{n+3}, \mathbb{R}^n\right)$ and $\beta_2 \in C^1\left(\mathbb{R}^{n+4}, \mathbb{R}^n\right)$ such that ϕ_2 is left-invertible with respect to x and the C^1 manifold

$$\mathcal{M}_2 := \left\{(y, x, \hat{y}, \xi, u, t) \in \mathbb{R}^{2n+4} | y = \hat{y},\ \phi_2(x, y, u, t) = \beta_2(\hat{y}, \xi, y, u, t)\right\} \tag{32}$$

satisfies the properties P1 and P2 with respect to systems (6) and (31) for all $(y, x, \hat{y}, \xi, u, t) \in \mathcal{X}_2 \times \mathbb{R}_{\geq 0}$ where $\mathcal{X}_2 \subset \Omega_{\text{ext}} \times \mathbb{R}^{n+1} \times [-u_0, u_0]$ is a connected $2n + 3$-dimensional manifold.

Remark 6. According to Definition 4, $\hat{y}$ is an asymptotic estimate of the measured state, y. Moreover, assuming that ϕ_2^L is a left-inverse of the mapping ϕ_2, an asymptotically convergent estimate of the unmeasured state variables is given by

$$\hat{x} = \phi_2^L\left(\beta_2(\hat{y}, \xi, y, u, t), y, u, t\right). \tag{33}$$

As in the reduced-order case, the presence of the unknown function $h(.)$ hinders the application of Definition 4 to the full-order ESO design. Hence, we present the following definition.

Definition 5 (Full-order ESO). Consider the mathematical setting of Definitions 1 and 4; replace the properties P1 and P2 of the manifold $\mathcal{M}_2$ with the property P3 of Λ_r-attractivity for some $r_0 > 0$. Moreover, assume that for any positive $r_1 < r_0$ there exist design parameters that render $\mathcal{M}_2$ Λ_r-attractive. Then, system (31) is called a full-order ESO for the extended system (6).

In order to include an estimation error feedback in the ESO design, by defining

$$\tilde{y} := y - \hat{y}, \tag{34}$$

we assume that the manifold $\mathcal{M}_2$ takes the following form:

$$\mathcal{M}_2 := \left\{ (y, x, \hat{y}, \xi, u, t) \in \mathbb{R}^{2n+4} | \tilde{y} = 0,\ x - \eta_2 (\xi, \tilde{y}, u, t) = 0 \right\}, \tag{35}$$

where $\eta_2 \in C^1 \left(\mathbb{R}^{n+3}, \mathbb{R}^n \right)$. Accordingly, we introduce the following off-the-manifold coordinates;

$$\begin{aligned} z_1 &:= \tilde{y}, \\ z_2 &:= x - \eta_2 (\xi, \tilde{y}, u, t), \end{aligned} \tag{36}$$

Remark 7. By Remark 6, we have the asymptotic estimate $\hat{x} = \eta_2 (\xi, \tilde{y}, u, t)$, implying $x - \hat{x} = z_2$. Therefore, the off-the-manifold coordinates z_1 and z_2 correspond to the estimation errors of the measured and the unmeasured state variables, respectively.

Assumption 5. For all $(\xi, \tilde{y}, u, t) \in \mathbb{R}^{n+3}$, $\det(\partial \eta_2 / \partial \xi)$ is bounded away from zero.

According to the time derivatives of z_1 and z_2, and the invertibility of $(\partial \eta_2 / \partial \xi)$ by Assumption 5, we select the following dynamics for observer (31):

$$\begin{aligned} \alpha_1 (\hat{y}, \xi, y, u, t) &= C\eta_2 (\xi, \tilde{y}, u, t) + f_1 (y, u) + \varphi(z_1, t), \\ \alpha_2 (\hat{y}, \xi, y, u, t) &= \left(\frac{\partial \eta_2}{\partial \xi} \right)^{-1} \left(A\eta_2 (\xi, \tilde{y}, u, t) + \sum_{i=1}^{n-1} B_i f_{i+1} \left(y, \hat{\bar{x}}_i, u \right) + \frac{\partial \eta_2}{\partial \tilde{y}} \varphi(z_1, t) - \frac{\partial \eta_2}{\partial u} \dot{u} - \frac{\partial \eta_2}{\partial t} \right), \end{aligned} \tag{37}$$

where $\varphi \in C^1 (\mathbb{R} \times \mathbb{R}_{\geq 0}, \mathbb{R})$ is a design function, $\hat{x} = \eta_2 (\xi, \tilde{y}, u, t)$ and $\hat{\bar{x}}_i$ is defined componentwise according to $\hat{x}$. By (37), we have the off-the-manifold dynamics

$$\begin{aligned} \dot{z}_1(t) &= -\varphi(z_1(t), t) + Cz_2(t), \\ \dot{z}_2(t) &= \left(A - \frac{\partial \eta_2}{\partial \tilde{y}} C \right) z_2(t) + \sum_{i=1}^{n-1} B_i \left(f_{i+1} \left(y(t), \bar{x}_i(t), u(t) \right) - f_{i+1} \left(y(t), \hat{\bar{x}}_i(t), u(t) \right) \right) \\ &\quad + B_n h \left(y(t), x(t), u(t), w(t), \dot{w}(t) \right). \end{aligned} \tag{38}$$

Assumption 6. (i) There exist a positive definite matrix $P_2 \in \mathbb{R}^{n \times n}$ and a positive ϵ_2 such that the following matrix inequality holds for all $(\hat{y}, \xi, y, u, t) \in \mathbb{R}^{n+4}$;

$$P_2 \left(A - \frac{\partial \eta_2}{\partial \tilde{y}} C \right) + \left(A - \frac{\partial \eta_2}{\partial \tilde{y}} C \right)^\top P_2 + \frac{2}{\epsilon_2} P_2 \leq 0. \tag{39}$$

(ii) The design function $\varphi(.)$ is quadratically bounded from below such that

$$z_1 \varphi(z_1, t) \geq \frac{\varphi_0}{\epsilon_2} z_1^2, \tag{40}$$

for all $z_1 \in \mathbb{R}$, $t \in \mathbb{R}_{\geq 0}$, and a positive φ_0.

Theorem 2. *Consider the extended system (6) and assume that Assumptions 1, 2, 5, and 6 are satisfied. System (31) with dynamics (37) is a full-order ESO–in the sense of Definition 5–for system (6), and the corresponding asymptotic estimates of the measured and the unmeasured state variables are given by $\hat{y}$ and $\hat{x} = \eta_2(\xi, \tilde{y}, u, t)$, respectively.*

Proof. We give the proof by the following steps:

Step 1. By Assumption 6, we consider the positive definite function

$$V_2(z_1, z_2) := z_1^2 + z_2^\top P_2 z_2, \tag{41}$$

and define $\lambda_m := \min\{1, \lambda_{\min}(P_2)\}$ and $\lambda_M := \max\{1, \lambda_{\max}(P_2)\}$.

Step 2. In the $(\hat{y}, \xi)$ space, we consider a compact set of the form, $\Omega_{\hat{y}} \times \Omega_\xi \subset \mathbb{R}^{n+1}$ such that $\mathcal{X}_2 := \Omega_{\text{ext}} \times \Omega_{\hat{y}} \times \Omega_\xi \times [-u_0, u_0]$ satisfies $\mathcal{M}_2 \cap (\text{int}(\mathcal{X}_2) \times \mathbb{R}_{\geq 0}) \neq \emptyset$. Applying the same argument and geometric setting as the proof of Theorem 1, we consider $\mathcal{X}_2$ as the connected manifold of interest.

Step 3. Following the similar procedure as the proof of Theorem 1, assume that

$$\epsilon_2 < \epsilon_2' := \frac{2\lambda_{\min}(P_2)}{l_f \lambda_{\max}(P_2)} \left(1 + \sqrt{1 + \frac{\lambda_{\min}(P_2)}{\varphi_0 l_f^2 \lambda_{\max}^2(P_2)}}\right)^{-1}. \tag{42}$$

Accordingly, the time derivative of the function $V_2(z_1, z_2)$, along the trajectories of (38), satisfies

$$\dot{V}_2(z_1(t), z_2(t)) \leq -\frac{2}{\lambda_2(\epsilon_2)} V_2(z_1(t), z_2(t)) + 2h_0 \frac{\lambda_{\max}(P_2)}{\sqrt{\lambda_m}} \sqrt{V_2(z_1(t), z_2(t))}, \tag{43}$$

where

$$\lambda_2(\epsilon_2) := \lambda_M \lambda_{\min}^{-1}\left(\begin{bmatrix} \frac{\varphi_0}{\epsilon_2} & -\frac{1}{2} \\ -\frac{1}{2} & \frac{\lambda_{\min}(P_2)}{\epsilon_2} - l_f \lambda_{\max}(P_2) \end{bmatrix}\right). \tag{44}$$

We note that $\lambda_2 : [0, \epsilon_2') \to \mathbb{R}_{\geq 0}$ is a strictly increasing surjective function.

Employing the comparison lemma, we have

$$\|\text{col}(z_1(t), z_2(t))\| \leq \left(\sqrt{\frac{\lambda_M}{\lambda_m}} \|\text{col}(z_1(t_0), z_2(t_0))\| - h_0 \frac{\lambda_{\max}(P_2)}{\lambda_m} \lambda_2(\epsilon_2)\right) \exp\left(-\frac{t - t_0}{\lambda_2(\epsilon_2)}\right) + \frac{\lambda_{\max}(P_2)}{\lambda_m} \lambda_2(\epsilon_2) h_0, \tag{45}$$

for all $t_0 \in \mathbb{R}_{\geq 0}$, $t \geq t_0$. Now, assume that $\text{col}(z_1(t_0), z_2(t_0)) \in \Lambda_{r_0}$ where r_0 is a positive and consider the positive numbers r_1, r_2 that satisfy $r_2 < r_1 < r_0$. The boundedness of the trajectories starting in Λ_{r_0} follows from inequality (45). Consider the reaching time

$$t_r := \lambda_2(\epsilon_2) \ln\left(\frac{1}{r_2}\left|\sqrt{\frac{\lambda_M}{\lambda_m}} \|\text{col}(z_1(t_0), z_2(t_0))\| - \frac{\lambda_{\max}(P_2)}{\lambda_m} \lambda_2(\epsilon_2) h_0\right|\right). \tag{46}$$

Define $\epsilon_2'' < \epsilon_2'$ as the unique solution of the equation

$$\lambda_2(\epsilon_2'') := \frac{\lambda_m(r_1 - r_2)}{\lambda_{\max}(P_2) h_0}, \tag{47}$$

and let $\epsilon_2 < \epsilon_2''$. For all $t \geq t_0 + t_r$, we have $\text{col}(z_1(t), z_2(t)) \in \Lambda_{r_1}$. Therefore, the manifold $\mathcal{M}_2$ is Λ_r-attractive for any positive $r_1 < r_0$ and system (31) with dynamics (37) constitutes a full-order ESO for the extended system (6). ∎

Corollary 2. *If Theorem 2 holds, then* $\overline{\lim}_{\substack{t \to \infty \\ \epsilon_2 \to 0}} \|\text{col}(z_1(t), z_2(t))\| = 0$.

Proof. Considering inequality (45), we have

$$\overline{\lim_{t\to\infty}} \|\mathrm{col}\,(z_1(t), z_2(t))\| \leq \frac{\lambda_{\max}(P_2)}{\lambda_{\mathrm{m}}} \lambda_2(\epsilon_2) h_0. \tag{48}$$

By definition (44), $\lambda_2(\epsilon_2) = O(\epsilon_2)$ as $\epsilon_2 \to 0$; hence, the ultimate bound of $\|\mathrm{col}\,(z_1(.), z_2(.))\|$ goes to zero as $\epsilon_2 \to 0$. ∎

Remark 8. To compare the feedback mechanism of the proposed full-order ESO with conventional ESOs, we note that the observer dynamics can be written in the $(\hat{y}, \hat{x})$ coordinates as

$$\begin{aligned} \dot{\hat{y}} &= C\hat{x} + f_1\,(y, u) + \varphi(\tilde{y}, t), \\ \dot{\hat{x}} &= A\hat{x} + \sum_{i=1}^{n-1} B_i f_{i+1}\left(y, \hat{\bar{x}}_i, u\right) + \frac{\partial \eta_2}{\partial \tilde{y}} C\tilde{x}, \end{aligned} \tag{49}$$

where $\tilde{x} := x - \hat{x}$. This reveals that the observer, unlike conventional ones, takes feedback from the estimation errors $\tilde{x}$ in addition to $\tilde{y}$. Furthermore, by the off-the-manifold dynamics (38), we have $C\tilde{x} = \dot{\hat{y}} + \varphi(\tilde{y}, t)$. This implies that the proposed full-order ESO, in general, has a nonlinear proportional-derivative property.

5 | FURTHER RESULTS

In this section–in order to unify the presentation for both reduced-order and full-order ESOs–we drop the subscripts, and we denote the feedback variable by $\upsilon \in \mathbb{R}$ such that $\upsilon = y$ for the reduced-order ESO and $\upsilon = \tilde{y}$ for the full-order ESO.

5.1 | Convergence analysis via LMIs

Since Assumptions 4 and 6 are instrumental in the convergence results of Theorems 1 and 2, respectively, we propose an LMI-based method to verify these assumptions. Consider the ith component of $(\partial\eta/\partial\upsilon)(t)$, $a_i \in C^1\,(\mathbb{R}_{\geq 0}, \mathbb{R})$, and assume that the following assumption holds.

Assumption 7. The functions $a_i(.)$, $i = 1 : n$, are globally bounded in the sense that

$$a_i^{\min} \leq a_i(t) \leq a_i^{\max}, \tag{50}$$

for all $t \in \mathbb{R}_{\geq 0}$ and some known constants $a_i^{\min}, a_i^{\max} \in \mathbb{R}$.

Remark 9. Roughly speaking, Assumption 7 means that the ESO applies bounded gains on the feedback signal υ. This translates into the sector-boundedness of the ESO feedback function that processes υ.[5]

By Assumption 7, we obtain the following time-varying model for $a_i(.)$;

$$a_i(t) = a_i^0 + a_i^1 \theta_i(t), \tag{51}$$

where $a_i^0 := (a_i^{\max} + a_i^{\min})/2$, $a_i^1 := (a_i^{\max} - a_i^{\min})/2$, and $|\theta_i(t)| \leq 1$ for all $t \in \mathbb{R}_{\geq 0}$. According to model (51), we have the following norm-bounded representation;

$$A - \frac{\partial \eta}{\partial \upsilon}(t) C = A_0 + A_1 \Theta(t) A_2, \tag{52}$$

where

$$A_0 = \begin{bmatrix} -a_1^0 & 1 & 0 & \dots & 0 \\ -a_2^0 & 0 & 1 & \dots & 0 \\ \vdots & \vdots & \vdots & \ddots & \vdots \\ -a_{n-1}^0 & 0 & 0 & \dots & 1 \\ -a_n^0 & 0 & 0 & \dots & 0 \end{bmatrix} \in \mathbb{R}^{n\times n}, A_1 = [A_{11}, \dots, A_{1n}],\ A_{1j} = \begin{bmatrix} -a_1^1\delta_{1j} & 0 & 0 & \dots & 0 \\ -a_2^1\delta_{2j} & 0 & 0 & \dots & 0 \\ \vdots & \vdots & \vdots & \ddots & \vdots \\ -a_{n-1}^1\delta_{(n-1)j} & 0 & 0 & \dots & 0 \\ -a_n^1\delta_{nj} & 0 & 0 & \dots & 0 \end{bmatrix} \in \mathbb{R}^{n\times n},$$

$$\Theta(t) = \operatorname{diag}\big(\Theta_j(t)\big)_{j=1}^{n},\ \Theta_j(t) := \theta_j(t) I \in \mathbb{R}^{n\times n}, A_2 = [A_{21},\ \dots\ , A_{2n}]^\top, A_{2j} = \begin{bmatrix} 1 & 0 & 0 & \dots & 0 \\ 0 & 0 & 0 & \dots & 0 \\ \vdots & \vdots & \vdots & \ddots & \vdots \\ 0 & 0 & 0 & \dots & 0 \\ 0 & 0 & 0 & \dots & 0 \end{bmatrix} \in \mathbb{R}^{n\times n}. \tag{53}$$

Theorem 3. *Assume that the components of partial derivative $(\partial\eta/\partial\upsilon)$ satisfy Assumption 7, so that the norm-bounded model (52) is valid. For a given positives ϵ, assume that there exists a positive definite matrix $P \in \mathbb{R}^{n\times n}$ satisfying the LMI*

$$\begin{bmatrix} PA_0 + A_0^\top P + \frac{2}{\epsilon}P & PA_1 & A_2^\top \\ A_1^\top P & -I & O \\ A_2 & O & -I \end{bmatrix} \leq 0. \tag{54}$$

Then, Assumption 4 (Assumption 6) holds with the matrix $P_1 = P$ ($P_2 = P$) and the positive $\epsilon_1 = \epsilon$ ($\epsilon_2 = \epsilon$).

Proof. According the norm-bounded model (52), the matrix inequality (19) (or (39)) is rewritten as

$$P\,(A_0 + A_1\Theta(t)A_2) + (A_0 + A_1\Theta(t)A_2)^\top P + \frac{2}{\epsilon}P \leq 0. \tag{55}$$

Using Young's inequality[5] along with the constraint $\Theta^\top(t)\Theta(t) \leq I$, we have

$$PA_1\Theta(t)A_2 + A_2^\top\Theta^\top(t)A_1^\top P \leq \frac{1}{\mu}PA_1A_1^\top P + \mu A_2^\top A_2, \tag{56}$$

for any positive μ. Therefore, the inequality (56) holds if

$$PA_0 + A_0^\top P + \frac{2}{\epsilon}P + \frac{1}{\mu}PA_1A_1^\top P + \mu A_2^\top A_2 \leq 0. \tag{57}$$

According to Schur's complements and using the homogeneity in P and μ,[27] the inequality (57) is equivalent to the feasibility of the LMI (54) for a positive definite matrix P. ■

Remark 10. The minimum value of ϵ, denoted by $\epsilon_{\min}$, can be obtained by solving the following generalized eigenvalue problem (GEVP):[27]

$$\begin{aligned} &\text{minimize } -\frac{2}{\epsilon} \\ &\text{subject to } P > 0 \text{ and matrix inequality (54).} \end{aligned} \tag{58}$$

5.2 | Some remarks on the ESO design

In Section 4, we constructed a general framework for the ESO design. Now, we further examine this framework to obtain some particular design cases, and we show that it provides a fairly general setting for large classes of observer gains.

Remark 11. According to Equations (17) and (37), if the function $\eta(.)$ depends explicitly on the known input $u(.)$, the time-derivative $\dot{u}(.)$ appears in the observer dynamics. Since, from a practical point of view, differentiating a signal is not desirable, we set $\partial\eta/\partial u = 0$.

The dependence of the function $\eta(.)$ on the variable υ determines how the ESO dynamics processes the measurements. Moreover, according to the off-the-manifold dynamics (18) and (38), $\partial\eta/\partial\upsilon$ plays a key role in the convergence of the estimated states. Hence, we discuss some special cases regarding the design of $\partial\eta/\partial\upsilon$.

5.2.1 | Linear design

A simple design, as in the case of conventional linear ESOs, is to impose a linear structure on the dependence of the function $\eta(.)$ on the measurements. That is,

$$\frac{\partial \eta^{(i)}}{\partial \upsilon} = k_i, \tag{59}$$

where $\eta^{(i)}$ is the ith component of η and k_i, $i=1:n$, are positive numbers. According to (59) and Remark 11, we select

$$\eta^{(i)}(\xi, \upsilon) = k_i \upsilon + \varpi_i(\xi), \tag{60}$$

where the functions $\varpi_i \in C^1(\mathbb{R}^n, \mathbb{R})$ should be designed to satisfy Assumption 3 (or Assumption 5). We note that the design (59) trivially satisfies Assumption 7 and, since $\partial \eta^{(i)}/\partial \upsilon$ are constants, LMI (54) reduces to

$$PA_0 + A_0^\top P + \frac{2}{\epsilon} P \leq 0. \tag{61}$$

Using the standard eigenvalue assignment methods, it is always possible to obtain the positives k_i that guarantee the feasibility of LMI (61). As a result, GEVP (58) translates into

$$\begin{aligned} &\text{minimize } -\frac{2}{\epsilon} \\ &\text{subject to } P > 0 \text{ and matrix inequality (61).} \end{aligned} \tag{62}$$

Design function $\varphi(.)$: For a positive κ and $\epsilon \geq \epsilon_{\min}$, we set

$$\varphi(\upsilon) = \frac{\kappa}{\epsilon} \upsilon \tag{63}$$

that satisfies the quadratic bound (40) with $\varphi_0 = \kappa$.

5.2.2 | Nonlinear design

The linear design (59) provides a uniform constant distribution of the observer gain over $\upsilon \in \mathbb{R}$. To obtain the gain k_{i1} for $\upsilon \in [c_1, c_2]$ and the gain k_{i2} for $\upsilon \in \mathbb{R} \setminus [c_1, c_2]$, we propose the following nonlinear design:

$$\frac{\partial \eta^{(i)}}{\partial \upsilon} = \frac{k_{i2} - k_{i1}}{2} \left(\tanh\left(\frac{\upsilon - c_2}{d_0}\right) - \tanh\left(\frac{\upsilon - c_1}{d_0}\right) \right) + k_{i2}, \tag{64}$$

with d_0 being a small positive. By integrating (64), we obtain

$$\eta^{(i)}(\xi, \upsilon) = d_0 \frac{k_{i2} - k_{i1}}{2} \ln \left(\frac{\cosh\left(\frac{\upsilon - c_2}{d_0}\right)}{\cosh\left(\frac{\upsilon - c_1}{d_0}\right)} \right) + k_{i2}\upsilon + \varpi_i(\xi), \tag{65}$$

where the functions $\varpi_i \in C^1(\mathbb{R}^n, \mathbb{R})$ should be designed to satisfy Assumption 3 (or Assumption 5). We note that, by the nonlinear design (64), the terms $\partial \eta^{(i)}/\partial \upsilon$, $i=1:n$ are globally bounded and therefore, Assumption (7) holds. In addition, the lower and the upper bounds of inequality (50) are given by $a_i^{\min} = \min\{k_{i1}, k_{i2}\}$ and $a_i^{\max} = \max\{k_{i1}, k_{i2}\}$, respectively. The nonlinear design (64) can improve the noise immunity of the ESO by producing smaller gains in certain ranges of the measurements.

Design function $\varphi(.)$: To obtain the gain κ_1/ϵ for $\upsilon \in [-c, c]$ and the gain $\kappa_2/\epsilon > \kappa_1/\epsilon$ for $\upsilon \in \mathbb{R} \setminus [-c, c]$, we set

$$\varphi(\upsilon) = d_0 \frac{\kappa_2 - \kappa_1}{2\epsilon} \ln\left(\frac{\cosh\left(\frac{\upsilon - c}{d_0}\right)}{\cosh\left(\frac{\upsilon + c}{d_0}\right)}\right) + \frac{\kappa_2}{\epsilon}\upsilon. \tag{66}$$

where $\epsilon \geq \epsilon_{\min}$. This nonlinear function satisfies the quadratic bound (40) with $\varphi_0 = \kappa_1$.

5.2.3 | Time-varying design

In both designs (59) and (64), it is possible to obtain faster convergence rates by selecting sufficiently large gains. However, it is well-known that large observer gains can result in the peaking phenomenon during the transient response.[9,28] One possible remedy for this issue is to apply a smaller observer gain during the transient phase and a larger observer gain in the steady-state.[9] Following this idea, we modify the nonlinear design (64) to include time-varying gains;

$$\frac{\partial \eta^{(i)}}{\partial \upsilon} = \frac{\overline{k}_{i2}(t) - \overline{k}_{i1}(t)}{2}\left(\tanh\left(\frac{\upsilon - c_2}{d_0}\right) - \tanh\left(\frac{\upsilon - c_1}{d_0}\right)\right) + \overline{k}_{i2}(t), \tag{67}$$

where

$$\overline{k}_{ij}(t) = 1 + (k_{ij} - 1)\tanh\left(\frac{t}{d_1}\right),\ j = 1, 2, \tag{68}$$

with d_1 being a positive number. The functions (68) provide a smooth transition of the gain values from 1 to the desired values k_{i1}, k_{i2}. A rough estimate of the transition time is given by $2d_1$; therefore, faster gain transitions can be obtained by selecting smaller values of d_1. According to (67), we have

$$\eta^{(i)}(\xi, \upsilon, t) = d_0 \frac{\overline{k}_{i2}(t) - \overline{k}_{i1}(t)}{2} \ln\left(\frac{\cosh\left(\frac{\upsilon - c_2}{d_0}\right)}{\cosh\left(\frac{\upsilon - c_1}{d_0}\right)}\right) + \overline{k}_{i2}(t)\upsilon + \varpi_i(\xi), \tag{69}$$

where the functions $\varpi_i \in C^1(\mathbb{R}^n, \mathbb{R})$ should be designed to satisfy Assumption 3 (or Assumption 5). The time-varying design (67) satisfies Assumption 7. In general, the lower and the upper bounds of inequality (50) are given by $a_i^{\min} = \min\{1, k_{i1}, k_{i2}\}$ and $a_i^{\max} = \max\{1, k_{i1}, k_{i2}\}$, respectively. However, these bounds tend to result in conservative solutions to GEVP (58). Hence, more accurate solution can be obtained using the bounds $a_i^{\min} = \min\{\overline{k}_{i1}(2d_1), \overline{k}_{i2}(2d_1)\}$ and $a_i^{\max} = \max\{k_{i1}, k_{i2}\}$, which are valid for $t > 2d_1$. We note that–in design (67)–the partial derivative $\partial\eta/\partial t$, which appears in the ESO dynamics (17) and (37), is no longer zero but it is given by

$$\frac{\partial \eta^{(i)}}{\partial t} = d_0 \frac{\dot{\overline{k}}_{i2}(t) - \dot{\overline{k}}_{i1}(t)}{2} \ln\left(\frac{\cosh\left(\frac{\upsilon - c_2}{d_0}\right)}{\cosh\left(\frac{\upsilon - c_1}{d_0}\right)}\right) + \dot{\overline{k}}_{i2}(t)\upsilon, \tag{70}$$

where $\dot{\overline{k}}_{ij}(t)$ is the time derivative of $\overline{k}_{ij}(t), j = 1, 2$.

Design function $\varphi(.)$: The time-varying version of the nonlinear function (66) is given by

$$\varphi(\upsilon, t) = d_0 \frac{\overline{\kappa}_2(t) - \overline{\kappa}_1(t)}{2\epsilon} \ln\left(\frac{\cosh\left(\frac{\upsilon - c}{d_0}\right)}{\cosh\left(\frac{\upsilon + c}{d_0}\right)}\right) + \frac{\overline{\kappa}_2(t)}{\epsilon}\upsilon, \tag{71}$$

where

$$\overline{\kappa}_j(t) = 1 + (\kappa_j - 1)\tanh\left(\frac{t}{d_1}\right), \; j = 1, 2. \tag{72}$$

This time-varying nonlinear function satisfies the quadratic bound (40) with $\varphi_0 = \overline{\kappa}_1(2d_1)$, for $t > 2d_1$. We note that similar time-varying gains can be applied to the linear designs (59) and (63).

6 | SIMULATION EXAMPLE

To show the efficacy of the proposed ESO design, we consider the following second-order system:[9]

$$\begin{aligned}
\dot{\zeta}_1(t) &= \zeta_2(t) + f_1(\zeta_1(t), u(t)), \\
\dot{\zeta}_2(t) &= f_2(\zeta_1(t), \zeta_2(t), u(t)) + g(\zeta_1(t), \zeta_2(t), w(t)),
\end{aligned} \tag{73}$$

where ζ_1 and ζ_2 are the state variables and

$$\begin{aligned}
f_1(\zeta_1, u) &= u\sin(\zeta_1), \\
f_2(\zeta_1, \zeta_2, u) &= u\sin(\zeta_2), \\
g(\zeta_1, \zeta_2, w) &= -2\zeta_1 - 4\zeta_2 + w + \cos(\zeta_1 + \zeta_2 + w).
\end{aligned} \tag{74}$$

The known and the disturbance inputs are considered as $u(t) = 1 + \sin(t)$ and $w(t) = \sin(2t + 1)$, respectively. The initial values of the state variables are $\zeta_1(0) = 1$ and $\zeta_2(0) = 1$. In the reduced-order ESO, the objective is to estimate the unmeasured state $x_1 = \zeta_2$ and the total disturbance $x_2 = g(\zeta_1, \zeta_2, w)$ using the measurement $y = \zeta_1$ and the known input u. In the full-order ESO, the measured state y is estimated as well. Owing to the stable linearized dynamics around the origin and bounded inputs, by confining the initial conditions to a compact set, system (73) satisfies Assumption 1. In order to investigate the effect of measurement noise, we add a high-frequency signal, $0.001\sin(100\pi t)$ to the measured output y. Simulations were done in the MATLAB/Simulink environment using the fourth-order Runge–Kutta method with a discretization step of 0.001. For each design, the corresponding GEVP (58) is solved by MATLAB's LMI solver.[29] We now consider the three designs discussed in Section 5, and, for simplicity, we set $\varpi_i(\xi) = \xi_i$.

- *Linear design*: According to Equation (60), to place the eigenvalues of the matrix A_0 on -10, we select the gains as $k_1 = 20$ and $k_2 = 100$. Through solving GEVP (62), we have

$$P = \begin{bmatrix} 11.7926 & -1.6415 \\ -1.6415 & 0.2894 \end{bmatrix}, \; \epsilon_{\min} = 0.1. \tag{75}$$

  In the case of the full-order ESO, the linear function (63) is used with the gain $\kappa = 10\epsilon_{\min}$.

- *Nonlinear design*: By Equation (65), following the intuitive idea of placing the eigenvalues of the matrix $A - (\partial\eta/\partial y)C$ on -5 within the desired interval and on -10 elsewhere, we select the gains as $k_{11} = 10$, $k_{12} = 20$, $k_{21} = 25$, and $k_{22} = 100$ with $d_0 = 0.1$. The desired intervals are selected as $[1, 1.5]$ and $[-0.3, 0.3]$ for the reduced-order and full-order ESOs, respectively. By solving GEVP (58), we obtain

$$P = \begin{bmatrix} 0.3500 & -0.0250 \\ -0.0250 & 0.0042 \end{bmatrix}, \; \epsilon_{\min} = 1.5487. \tag{76}$$

  In the case of the full-order ESO, we use the nonlinear function (66) with gains $\kappa_1 = 5\epsilon_{\min}$, $\kappa_2 = 10\epsilon_{\min}$ and the desired interval $[-0.3, 0.3]$.

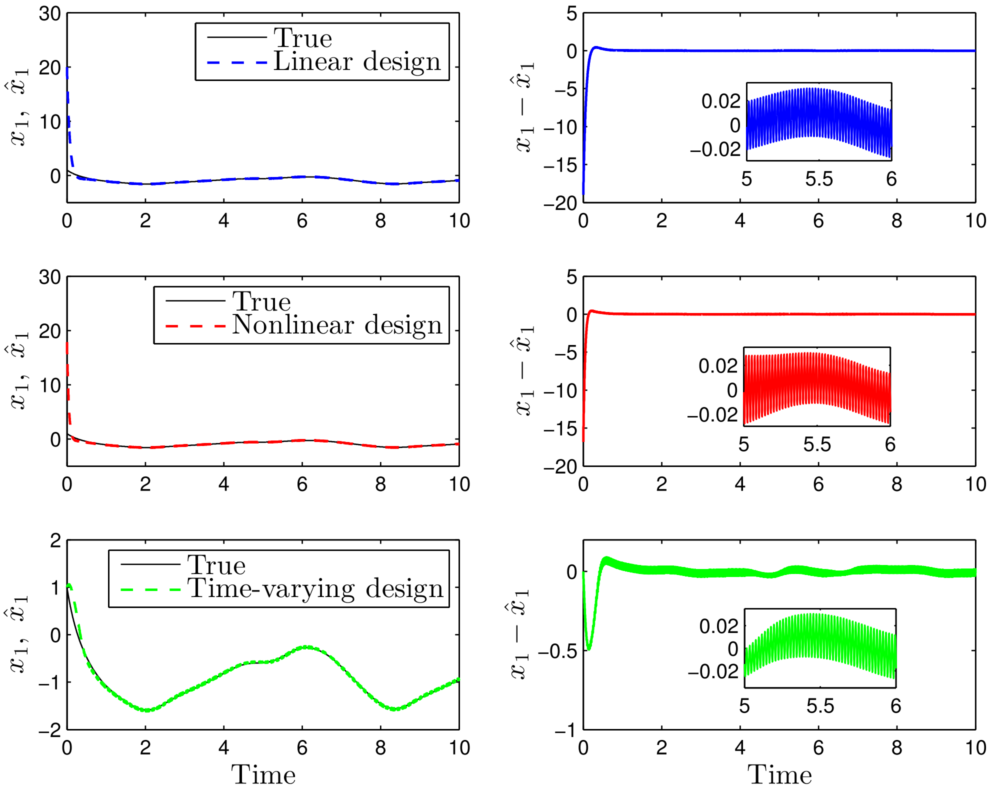

FIGURE 1 Estimation of state variable x_1 using reduced-order extended state observer [Colour figure can be viewed at wileyonlinelibrary.com]

- *Time-varying design*: We consider the nonlinear design with the difference that the parameters vary with respect to time as

$$\overline{k}_{ij}(t) = 1 + (k_{ij} - 1)\tanh(10t),$$
$$\overline{\kappa}_j(t) = 1 + (\kappa_j - 1)\tanh(10t). \tag{77}$$

Considering $t > 0.2$, the solution of GEVP (58) is obtained as

$$P = \begin{bmatrix} 0.3202 & -0.0230 \\ -0.0230 & 0.0041 \end{bmatrix},\ \epsilon_{\min} = 1.7266. \tag{78}$$

The estimation results of the reduced-order and full-order ESOs are shown in Figures 1–2 and 3–5, respectively. The mean and root mean square (RMS) values of the estimation errors are given in Table 1. These results confirm the convergence of state estimates for both reduced-order and full-order ESOs. Moreover, we observe that

1. The linear design produces a better estimate of the measured state y (in terms of mean and RMS values) because of the faster rate of convergence. However, the nonlinear design reduces the energy of the estimation errors for the state variables x_1 and x_2. This underlines the robustness of the nonlinear design against measurement noise amplification in higher-order derivatives of y.
2. The time-varying design alleviates the peaking phenomenon during the transient response. This, in turn, considerably improves the statistical properties of the estimation errors of x_1 and x_2.

6.1 | Comparison with conventional ESO

In this section, we provide a comparison between our proposed full-order ESO and a conventional ESO. For simplicity, we consider only the linear design. For system (73), the conventional linear ESO is given by

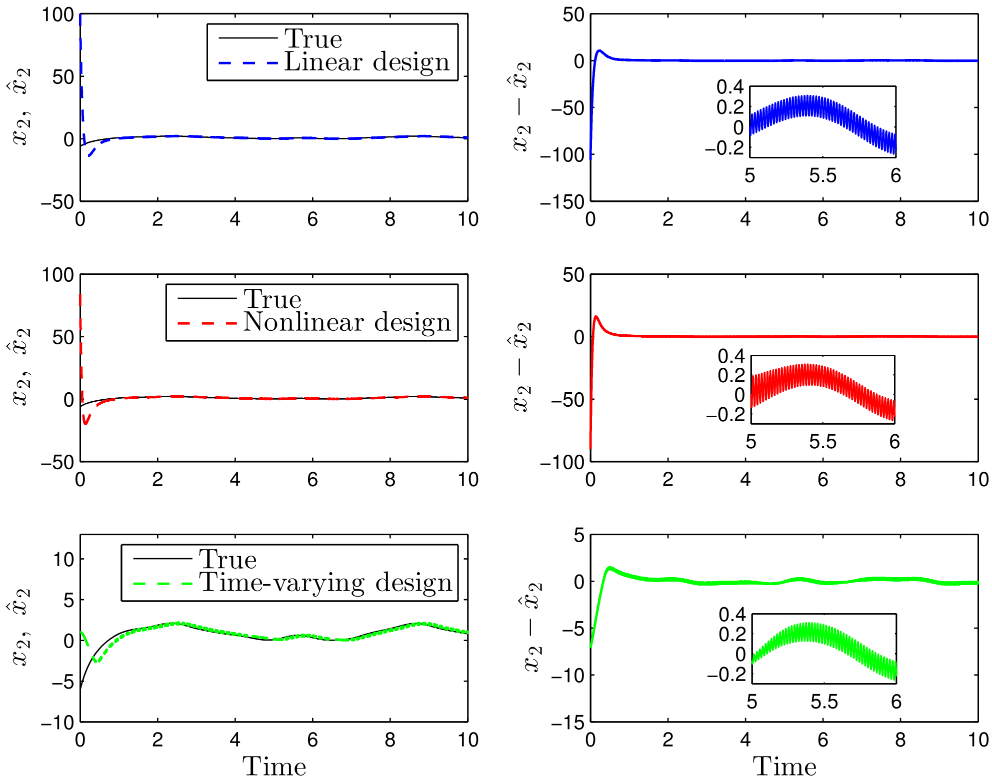

FIGURE 2 Estimation of state variable x_2 using reduced-order extended state observer [Colour figure can be viewed at wileyonlinelibrary.com]

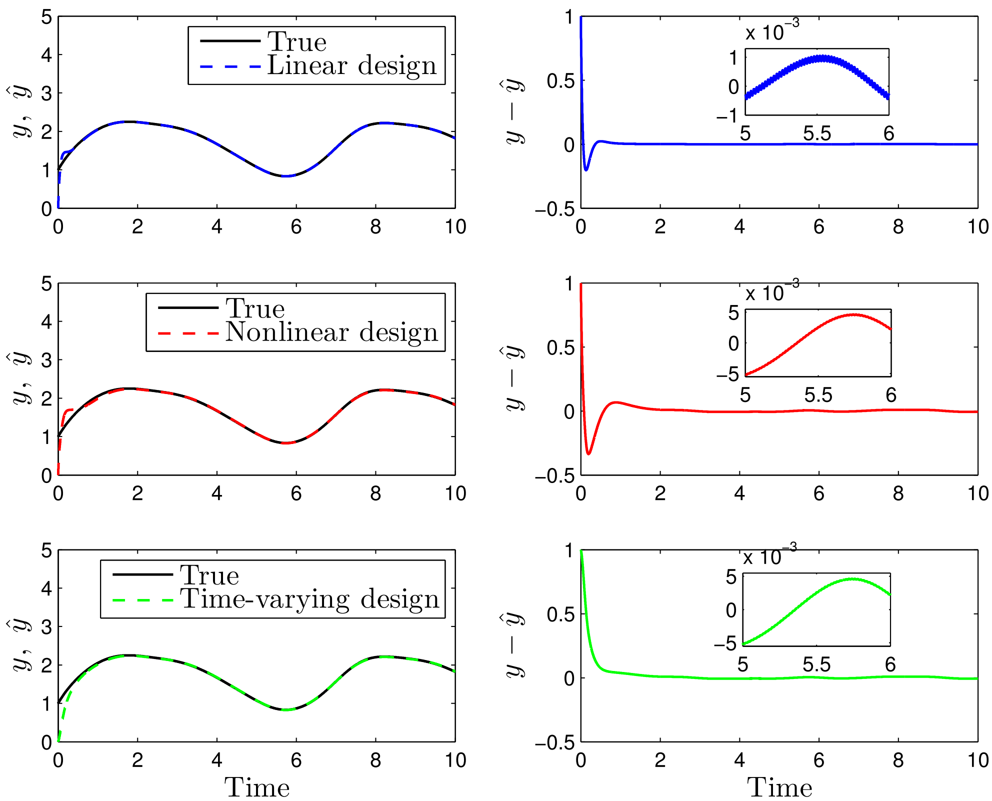

FIGURE 3 Estimation of state variable y using full-order extended state observer [Colour figure can be viewed at wileyonlinelibrary.com]

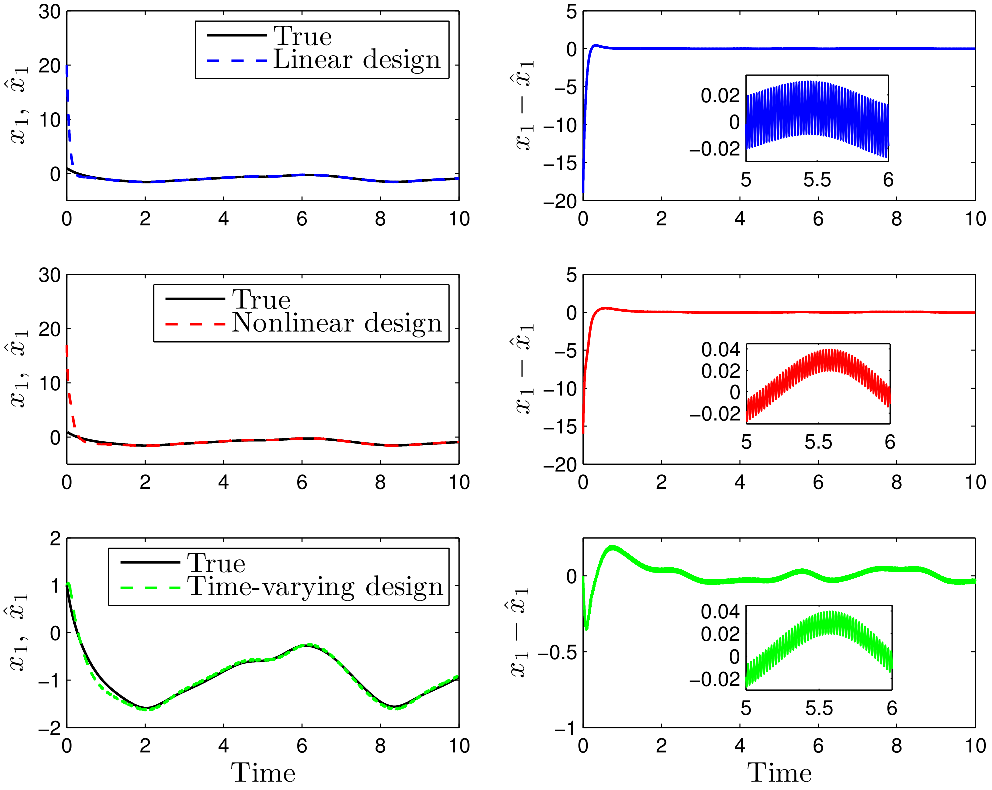

FIGURE 4 Estimation of state variable x_1 using full-order extended state observer [Colour figure can be viewed at wileyonlinelibrary.com]

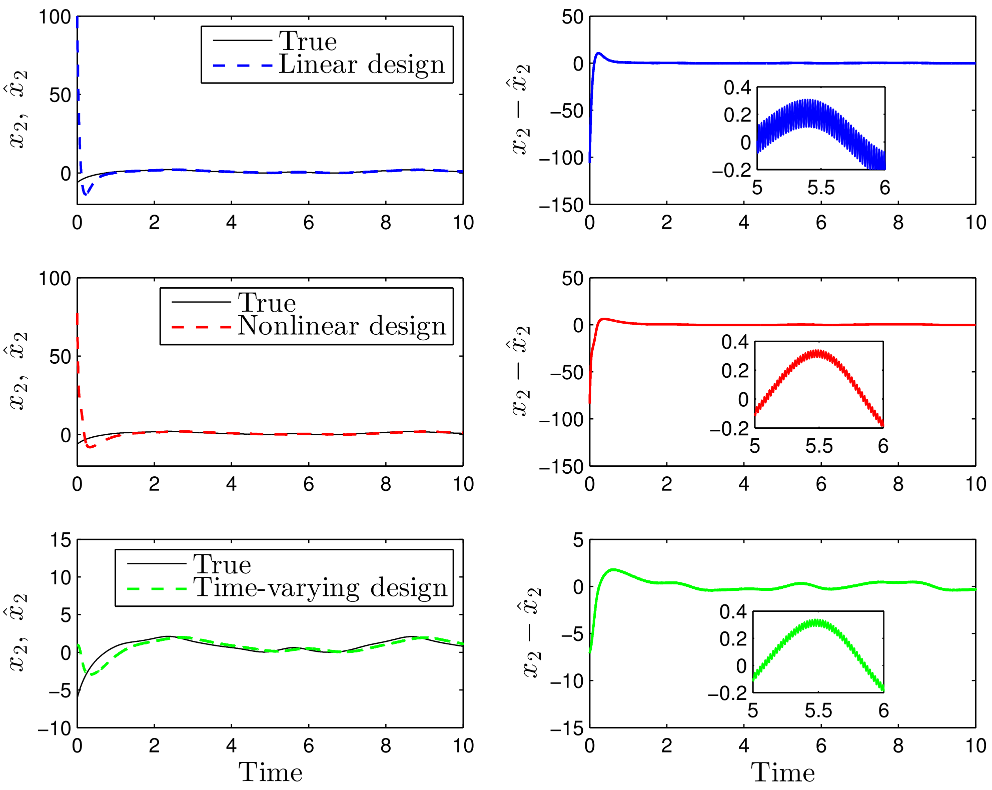

FIGURE 5 Estimation of state variable x_2 using full-order extended state observer [Colour figure can be viewed at wileyonlinelibrary.com]

TABLE 1 Statistical properties of ESO estimation errors

Reduced-order ESO	Linear design		Nonlinear design		Time-varying design	
	Mean value	RMS value	Mean value	RMS value	Mean value	RMS value
$x_1 - \hat{x}_1$	−0.1000	1.0854	−0.0523	0.7980	−0.0103	0.0720
$x_2 - \hat{x}_2$	−0.1098	5.4622	0.2075	4.1102	−0.0506	0.8129
Full-order ESO	**Linear design**		**Nonlinear design**		**Time-varying design**	
	Mean value	**RMS value**	**Mean value**	**RMS value**	**Mean value**	**RMS value**
$y - \hat{y}$	1.5482×10^{-4}	0.0441	-5.4979×10^{-4}	0.0655	0.0228	0.1039
$x_1 - \hat{x}_1$	−0.1000	1.0854	−0.1015	1.0346	0.0999	0.0680
$x_2 - \hat{x}_2$	−0.1098	5.4622	−0.1282	4.6359	0.0659	0.8416

Abbreviations: ESO, extended state observer; RMS, root mean square.

$$\begin{aligned}
\dot{\hat{y}} &= \hat{x}_1 + f_1(\hat{y}, u) + l_1\tilde{y},\\
\dot{\hat{x}}_1 &= \hat{x}_2 + f_2(\hat{y}, \hat{x}_1, u) + l_2\tilde{y},\\
\dot{\hat{x}}_2 &= l_3\tilde{y},
\end{aligned} \tag{79}$$

with design gains $l_1, l_2, l_3 > 0$. For linear full-order ESO, target manifold (35) reduces to

$$\mathcal{M}_2 = \left\{(y, x_1, x_2, \hat{y}, \xi_1, \xi_2) \in \mathbb{R}^6 | \tilde{y} = 0,\ x_1 = \xi_1 + k_1\tilde{y},\ x_2 = \xi_2 + k_2\tilde{y}\right\}, \tag{80}$$

resulting in the asymptotic estimates $\hat{x}_1 = \xi_1 + k_1\tilde{y}$ and $\hat{x}_2 = \xi_2 + k_2\tilde{y}$. The ESO dynamics, in $(\hat{y}, \hat{x})$ coordinates, satisfies

$$\begin{aligned}
\dot{\hat{y}} &= \hat{x}_1 + f_1(y, u) + \kappa\tilde{y},\\
\dot{\hat{x}}_1 &= \hat{x}_2 + f_2(y, \hat{x}_1, u) + k_1\tilde{x}_1,\\
\dot{\hat{x}}_2 &= k_2\tilde{x}_1,
\end{aligned} \tag{81}$$

As pointed out in Remark 8, the proposed ESO has a different feedback mechanism than that of the conventional one. To draw a fair comparison, we proceed as follows. The eigenvalues of the error dynamics, for each ESO, are all placed on ℓ. That is, $l_1 = 3\ell$, $l_2 = 3\ell^2$, and $l_3 = \ell^3$ for (79), and $\kappa = \ell$, $k_1 = 2\ell$, and $k_2 = \ell^2$ for (81). For each ESO, we find the optimal ℓ by solving the optimization problem

$$\begin{aligned}
\ell_{\text{opt}} &:= \arg\min_{\ell > 0} J(T),\\
J(T) &:= \sqrt{\frac{1}{T}\int_0^T \left(\frac{1}{5}\tilde{y}^2(\tau) + \frac{2}{5}\tilde{x}_1^2(\tau) + \frac{2}{5}\tilde{x}_2^2(\tau)\right) \mathrm{d}\tau},
\end{aligned} \tag{82}$$

where $T > 0$ is the simulation time. In the performance index $J(T)$, we put more weights on the estimation errors of the unmeasured state variables. Via bisection search, we obtain the following optimal values:

- For conventional ESO (79): $\ell_{\text{opt}} = 3.375$, $J_{\text{opt}}(10) = 1.1409$;
- For proposed ESO (81): $\ell_{\text{opt}} = 1.5313$, $J_{\text{opt}}(10) = 1.0152$.

The comparative results of estimation errors of both ESOs are given in Figure 6 and Table 2. The conventional ESO has a better performance in estimating y, while the proposed ESO, especially in terms of energy, shows a better performance in estimating x_1 and x_2.

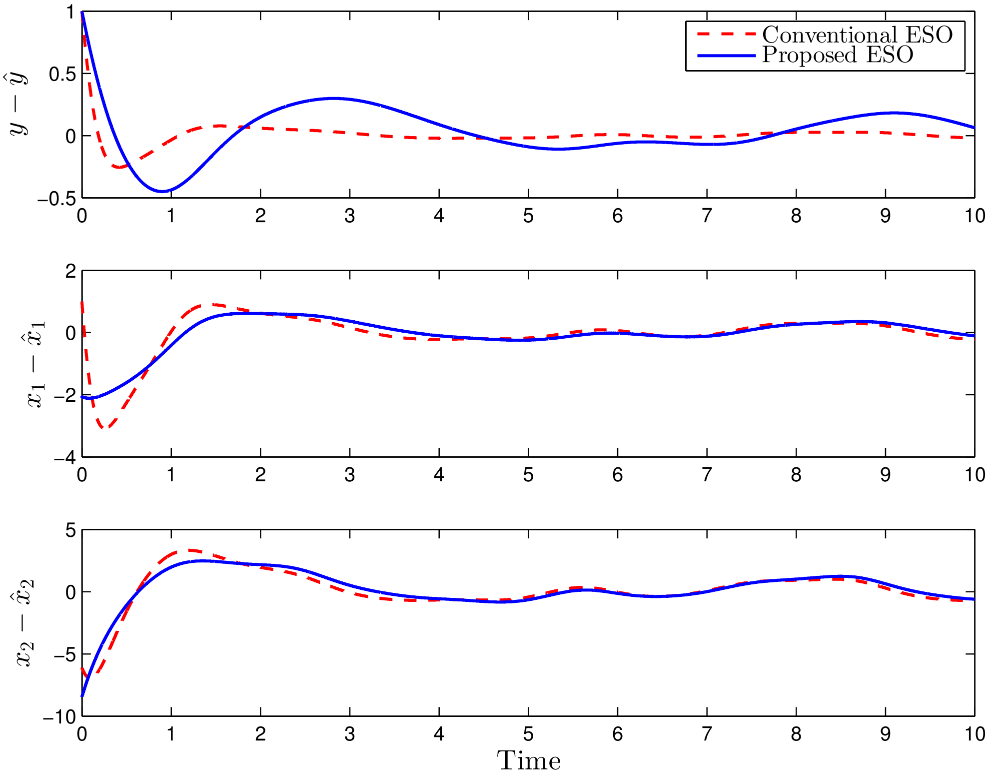

FIGURE 6 Estimation errors of conventional extended state observer (ESO) and proposed full-order ESO [Colour figure can be viewed at wileyonlinelibrary.com]

TABLE 2 Statistical properties of estimation errors of conventional ESO and proposed full-order ESO

	Conventional ESO		Proposed ESO	
Error variable	**Mean value**	**RMS value**	**Mean value**	**RMS value**
$y - \hat{y}$	0.0040	0.0906	0.0354	0.2016
$x_1 - \hat{x}_1$	−0.0575	0.7039	−0.0397	0.5746
$x_2 - \hat{x}_2$	0.1653	1.6602	0.2384	1.4931

Abbreviations: ESO, extended state observer; RMS, root mean square.

7 | CONCLUSION

This article studied the problem of ESO design for lower-triangular nonlinear systems using the I&I method. A novel geometric framework was developed for the design and convergence analysis of ESOs based on the concept of an attractive manifold. It was shown that this framework unifies the design and analysis of nonlinear and/or time-varying ESOs as remedies for the peaking phenomenon and measurement noise sensitivity. Rigorous numerical simulations were provided to support the theoretical results. Some potential future directions of this research are:

1. extending the ESO design to the case where all state equations of system (3) are perturbed by disturbances,
2. further investigation of the issue of measurement noise amplification,
3. studying the implications of the I&I formulation of ESOs in ADRC problems.

ACKNOWLEDGMENTS
This research has been supported by the University of Tabriz's Research office.

CONFLICT OF INTEREST
The authors declare no potential conflict of interests.

DATA AVAILABILITY STATEMENT

The data that support the findings of this study are available from the corresponding author upon reasonable request.

ORCID

Mehran Hosseini-Pishrobat https://orcid.org/0000-0002-5866-5131
Jafar Keighobadi https://orcid.org/0000-0002-1216-4518
Mohammad Javad Yazdanpanah https://orcid.org/0000-0001-7098-8331

REFERENCES

1. Han J. From PID to active disturbance rejection control. *IEEE Trans Ind Electron*. 2009;56(3):900-906. https://doi.org/10.1109/TIE.2008.2011621.
2. Gao Z. On the centrality of disturbance rejection in automatic control. *ISA Trans*. 2014;53(4):850-857. https://doi.org/10.1016/j.isatra.2013.09.012.
3. Zhao ZL, Guo BZ. On convergence of nonlinear active disturbance rejection control for SISO nonlinear systems. *J Dyn Control Syst*. 2016;22(2):385-412. https://doi.org/10.1007/s10883-015-9304-5.
4. Feng H, Guo BZ. Active disturbance rejection control: old and new results. *Annu Rev Control*. 2017;44:238-248. https://doi.org/10.1016/j.arcontrol.2017.05.003.
5. Hosseini-Pishrobat M, Keighobadi J. Robust output regulation of a triaxial MEMS gyroscope via nonlinear active disturbance rejection. *Int J Robust Nonlinear Control*. 2018;28(5):1830-1851. https://doi.org/10.1002/rnc.3983.
6. Hosseini-Pishrobat M, Keighobadi J. Extended state observer-based robust non-linear integral dynamic surface control for triaxial MEMS gyroscope. *Robotica*. 2019;37(3):481-501. https://doi.org/10.1017/S0263574718001133.
7. Guo BZ, Zhao Z. On the convergence of an extended state observer for nonlinear systems with uncertainty. *Syst Control Lett*. 2011;60(6):420-430. https://doi.org/10.1016/j.sysconle.2011.03.008.
8. Li J, Xia Y, Qi X, Wan H. On convergence of the discrete-time nonlinear extended state observer. *J Frankl Inst*. 2018;355(1):501-519. https://doi.org/10.1016/j.jfranklin.2017.11.019.
9. Zhao ZL, Guo BZ. Extended state observer for uncertain lower triangular nonlinear systems. *Syst Control Lett*. 2015;85:100-108. https://doi.org/10.1016/j.sysconle.2015.09.004.
10. Zhao ZL, Guo BZ. A nonlinear extended state observer based on fractional power functions. *Automatica*. 2017;81:286-296. https://doi.org/10.1016/j.automatica.2017.03.002.
11. Zhao ZL, Guo BZ. A novel extended state observer for output tracking of MIMO systems with mismatched uncertainty. *IEEE Trans Autom Control*. 2018;63(1):211-218. https://doi.org/10.1109/TAC.2017.2720419.
12. Astolfi A, Ortega R. Immersion and invariance: a new tool for stabilization and adaptive control of nonlinear systems. *IEEE Trans Autom Control*. 2003;48(4):590-606. https://doi.org/10.1109/TAC.2003.809820.
13. Astolfi A, Karagiannis D, Ortega R. *Nonlinear and Adaptive Control with Applications*. London, UK: Communications and Control Engineering London, Springer; 2008.
14. Karagiannis D, Carnevale D, Astolfi A. Invariant manifold based reduced-order observer design for nonlinear systems. *IEEE Trans Autom Control*. 2008;53(11):2602-2614. https://doi.org/10.1109/TAC.2008.2007045.
15. Yi B, Ortega R, Zhang W. On state observers for nonlinear systems: a new design and a unifying framework. *IEEE Trans Autom Control*. 2018;64(3):1193-1200. https://doi.org/10.1109/TAC.2018.2839526.
16. Tavan M, Khaki-Sedigh A, Arvan MR, Vali AR. Immersion and invariance adaptive velocity observer for a class of Euler–Lagrange mechanical systems. *Nonlinear Dyn*. 2016;85(1):425-437. https://doi.org/10.1007/s11071-016-2696-2.
17. Astolfi A, Ortega R, Venkatraman A. A globally exponentially convergent immersion and invariance speed observer for mechanical systems with non-holonomic constraints. *Automatica*. 2010;46(1):182-189. https://doi.org/10.1016/j.automatica.2009.10.027.
18. Khan IU, Wagg D, Sims ND. Nonlinear robust observer design using an invariant manifold approach. *Control Eng Pract*. 2016;55:69-79. https://doi.org/10.1016/j.conengprac.2016.06.015.
19. Keighobadi J, Hosseini-Pishrobat M, Faraji J, Langehbiz MN. Design and experimental evaluation of immersion and invariance observer for low-cost attitude-heading reference system. *IEEE Trans Ind Electron*. 2020;67(9):7871-7878.
20. Murguia C, Fey RH, Nijmeijer H. Immersion and invariance observers with time-delayed output measurements. *Commun Nonlinear Sci Numer Simul*. 2016;30(1-3):227-235. https://doi.org/10.1016/j.cnsns.2015.06.005.
21. Khalil HK. *Nonlinear Control*. Boston, MA: Pearson; 2015.
22. Ishijima S, Kojima A. Practical stabilization of nonlinear control systems. *IFAC Proc Vol*. 1992;25(21):216-219. https://doi.org/10.1016/S1474-6670(17)49755-2.
23. Gauthier JP, Kupka I. *Deterministic Observation Theory and Applications*. 1st ed. Cambridge, MA: Cambridge University Press; 2001.
24. Bernard P, Praly L, Andrieu V, Hammouri H. On the triangular canonical form for uniformly observable controlled systems. *Automatica*. 2017;85:293-300. https://doi.org/10.1016/j.automatica.2017.07.034.
25. Bernard P. *Observer Design for Nonlinear Systems. Volume 479 of Lecture Notes in Control and Information Sciences*. Cham, Switzerland: Springer International Publishing; 2019.
26. Lévine J. *Introduction to Differential Geometry*. Berlin/Heidelberg, Germany: Springer; 2009:13-41.

27. Boyd S, Ghaoui LE, Feron E, Balakrishnan V. *Linear Matrix Inequalities in System and Control Theory*. Studies in Applied Mathematics. Philadelphia, PA: Society for Industrial and Applied Mathematics; 1994.
28. Khalil HK. *High-Gain Observers in Nonlinear Feedback Control*. Philadelphia, PA: Society for Industrial and Applied Mathematics; 2017.
29. Gahinet P, Nemirovski A, Laub A, Chilali M. *LMI Control Toolbox: For Use with MATLAB*. Natick, MA: The MathWorks, Inc; 1995.

How to cite this article: Hosseini-Pishrobat M, Keighobadi J, Pirastehzad A, Javad Yazdanpanah M. Immersion and invariance-based extended state observer design for a class of nonlinear systems. *Int J Robust Nonlinear Control*. 2021;1–22. https://doi.org/10.1002/rnc.5607